

Validation of the Hsp70–Bag3 Protein–Protein Interaction as a Potential Therapeutic Target in Cancer

Xiaokai Li¹, Teresa Colvin², Jennifer N. Rauch¹, Diego Acosta-Alvear³, Martin Kampmann⁴, Bryan Dunyak¹, Byron Hann⁵, Blake T. Aftab⁵, Megan Murnane⁵, Min Cho⁴, Peter Walter³, Jonathan S. Weissman⁴, Michael Y. Sherman², and Jason E. Gestwicki¹

Abstract

Hsp70 is a stress-inducible molecular chaperone that is required for cancer development at several steps. Targeting the active site of Hsp70 has proven relatively challenging, driving interest in alternative approaches. Hsp70 collaborates with the Bcl2-associated athanogene 3 (Bag3) to promote cell survival through multiple pathways, including FoxM1. Therefore, inhibitors of the Hsp70–Bag3 protein–protein interaction (PPI) may provide a noncanonical way to target this chaperone. We report that JG-98, an allosteric inhibitor of

this PPI, indeed has antiproliferative activity (EC₅₀ values between 0.3 and 4 μmol/L) across cancer cell lines from multiple origins. JG-98 destabilized FoxM1 and relieved suppression of downstream effectors, including p21 and p27. On the basis of these findings, JG-98 was evaluated in mice for pharmacokinetics, tolerability, and activity in two xenograft models. The results suggested that the Hsp70–Bag3 interaction may be a promising, new target for anticancer therapy. *Mol Cancer Ther*; 14(3); 642–8. ©2015 AACR.

Introduction

HSP70 (Hsp70/HSPA1A) is a molecular chaperone that plays important roles in protein homeostasis and cell survival (1). It has become an attractive anticancer target based on expression data, knockdown studies, and the promising antiproliferative activity of first-generation inhibitors (2–8). However, the path toward safe and effective inhibitors of Hsp70 remains uncertain. One challenge is that the active site of Hsp70 is located in a deep groove in its nucleotide-binding domain (NBD). It has proven challenging to develop competitive inhibitors of this site, partly because of the tight affinity of Hsp70 for ATP (4). This observation has driven a search for noncanonical solutions (5, 9).

Hsp70 is known to collaborate with a wide range of cochaperones (9), including a family of proteins that contain conserved Bag domains, such as Bag1, Bag2, and Bag3. These Bag domains

bind to Hsp70 and help guide its chaperone functions. Of these cochaperones, Bag3 is of particular interest as an anticancer target because it is selectively upregulated in response to stress (10) and its expression is coelevated with Hsp70 in many tumor types (5, 11). Even more importantly, Bag3 has been shown to collaborate with Hsp70 in regulating cancer development through multiple pathways, including the cell cycle and suppression of oncogene-induced senescence (12). In line with these observations, blocking the Hsp70–Bag3 interaction using mutations, knockdowns, or first-generation small molecules has selective antiproliferative activity in cancer cells (12), suggesting that inhibiting the Hsp70–Bag3 protein–protein interaction (PPI) might be one noncanonical way to interrupt Hsp70 function.

Although initially daunting, numerous PPIs have emerged as promising drug targets in anticancer programs, with inhibitors of MDM2–p53 (13, 14), Mcl1–Bax (15), and others (16–18) being actively explored. There are many categories of PPIs, which are defined by the relative affinities of the protein partners and the amount of buried surface area in the complex (17, 19–21). The Hsp70–Bag3 interaction occurs with relatively tight affinity (~30 nmol/L), over a comparatively large surface area (22, 23), placing it in the category of a potentially difficult PPI to interrupt. However, PPIs with similar characteristics have been successfully inhibited using molecules that bind to allosteric sites (19, 20), suggesting that this PPI may be "druggable" with the right tool.

On the basis of these observations, we sought to explore whether the Hsp70–Bag3 interaction might be a suitable anticancer target using a newly identified, allosteric inhibitor, JG-98 (24). Here, we report that this molecule binds tightly to a conserved site on Hsp70 and weakens the Hsp70–Bag3 interaction *in vitro* and in cells. This compound had variable antiproliferative activity across a range of cancer cells (EC₅₀ ~ 0.3 to 4 μmol/L), but was relatively less toxic in healthy mouse fibroblasts (EC₅₀ ~ 4.5 μmol/L). JG-98 also disrupted the FoxM1

¹Department of Pharmaceutical Chemistry and the Institute for Neurodegenerative Disease, University of California at San Francisco, San Francisco, California. ²Department of Biochemistry, Boston University School of Medicine, Boston, Massachusetts. ³Department of Biochemistry and Biophysics, Howard Hughes Medical Institute, University of California at San Francisco, San Francisco, California. ⁴Department of Molecular and Cellular Pharmacology, Howard Hughes Medical Institute, University of California at San Francisco, San Francisco, California. ⁵Department of Medicine, Helen Diller Family Comprehensive Cancer Center, University of California at San Francisco, San Francisco, California.

Note: Supplementary data for this article are available at Molecular Cancer Therapeutics Online (<http://mct.aacrjournals.org/>).

Corresponding Author: Jason E. Gestwicki, University of California at San Francisco, 675 Nelson Rising Lane, San Francisco, CA 94158. Phone: 415-502-7121; E-mail: Jason.Gestwicki@ucsf.edu

doi: 10.1158/1535-7163.MCT-14-0650

©2015 American Association for Cancer Research.

cell-cycle pathway, consistent with the known roles of the Hsp70–Bag3 complex. Although JG-98 was not orally bioavailable, it was well tolerated in mice when delivered intraperitoneally and it suppressed tumor growth in two xenograft models. Together, these proof-of-concept studies suggest that the Hsp70–Bag3 interaction may be a promising target for further exploration.

Materials and Methods

Chemistry

YM-01, JG-98, and YM01-biotin were synthesized according to the previously published methods (24). The synthesis and characterization of JG98-biotin and the chemical structures of the molecules can be found in Supplementary Fig. S1.

Cells

MCF-7, MDA-MB-231, A375, MeWo, HeLa, HT-29, SKOV3, Jurkat, and mouse embryonic fibroblasts (MEF) were purchased from ATCC. Human multiple myeloma cell lines (MM1.R, INA6, RPMI-8226, JIN-3, U266, NCI-H929, L363, MM1.S, KMS11, LP-1, AMO-1, OPM1, and OPM2) stably transduced with a firefly luciferase expression vector were kindly provided by Dr. Constantine Mitsiades. All cells were cultured according to established protocols. Cell lines were not further authenticated.

Cell viability assays

MCF-7, MDA-MB-231, A375, MeWo, HeLa, HT-29, SKOV3, Jurkat, and MEF viabilities were determined by MTT cell proliferation assay kit from ATCC (ATCC number: 30–1010 K). Briefly, cells (2,000 per well for MEF and 5,000 per well for the others) were plated into 96-well TC-treated plates in 0.1 mL media and allowed to attach overnight. Cells were then treated with compounds with various concentrations in 0.2 mL media. The final DMSO concentration was 1%. After a 72-hour incubation in 5% CO₂, cells were washed three times with 0.1 mL PBS and then 0.1 mL fresh media with 10 μ L MTT reagents was added. The plates were incubated in dark and at 37°C for 4 hours, 0.1 mL detergent buffer was added into each well and the resulting solutions were quantified at an absorbance of 570 nm. Viability assays conducted in myeloma cell lines, stably transduced with firefly luciferase, were conducted as previously described (25, 26). Briefly, multiple myeloma cells were plated and treated with JG-98 at 11 concentrations, between 30 nmol/L and 30 μ mol/L, for 72 hours. Following incubation, luciferin substrate was added and bioluminescence signal was measured using a Biotek HT luminometer. Luminescence signal was normalized using mock treatment and no-cell controls as 100% and 0% viability references, respectively. IC₅₀ values were derived from dose–response curves plotted and fitted using Prism v.6.0c (GraphPad; see Supplementary Information).

Molecular docking

To facilitate docking studies, a molecular dynamics simulation was performed on Hsc70 NBD (PDB:3C7N) in GROMACS (v4.6.5). Coordinate and topology files for the NBD were prepared using the AMBER03 force-field and TIP3P water model. A rectangular box was generated that expanded 1.2 nm from the protein surface, filled with water molecules, and randomly populated with Na⁺/Cl[−] ions to an ionic strength of 100 mmol/L. The system was backbone restrained and energy minimized, followed by a two-step equilibration process to the target temperature and

pressure of 310 K and 1 bar. Backbone restraints were lifted and a full MD simulation was run for 5 ns with a 2-fs time step under constant pressure and temperature. A cluster analysis was performed to isolate the most representative conformation. We then performed docking studies using University of California at San Francisco, San Francisco, CA (UCSF Dock; v6.6). The receptor molecular surface was prepared with DMS, analyzed for potential-binding sites using Sphgen and a region of the NBD was chosen based on reported chemical shift perturbations from NMR titration studies (27). A box was generated surrounding the binding site by 6Å in all directions and the scoring grid was generated with GRID. Low-energy conformations of JG98 and YM-01 were prepared with Szybki and partial charges were calculated in UCSF Chimera using the AM1-BCC force field. Ligands were docked using the flex anchor-and-grow method. After initial pose generation and orientation in the binding site, ligands were rescored with AMBER using default scoring parameters for flexible ligand docking.

ELISA

ELISAs were carried out according to a previous published method (24). Briefly, Hsc70 was immobilized in ELISA well plates and treated with biotinylated compounds (see Supplementary Information). After washing, bound material was measured using streptavidin-horseradish peroxidase. Negative controls included wells lacking Hsc70 and JG98 lacking a biotin.

Flow cytometry protein interaction assay

Biotinylated Hsp72 was immobilized on polystyrene streptavidin-coated beads (Spherotech), incubated with Alexa-Fluor 488-labeled Bag1, Bag2, or Bag3 (50 nmol/L) and increasing amounts of JG-98 or YM-01 in buffer A (25 mmol/L HEPES, 5 mmol/L MgCl₂, 10 mmol/L KCl, 0.3% Tween-20 pH 7.5). Plates were incubated for 15 minutes then analyzed using a Hypercyt liquid sampling unit in line with an Accuri C6 Flow Cytometer. Protein complex inhibition was detected by measuring median bead-associated fluorescence. DMSO was used as a negative control and excess unlabeled Hsp70 (1 μ mol/L) was used as a positive control.

Coimmunoprecipitations

HeLa cell extracts were prepared in M-PER lysis buffer (Thermo Scientific) and adjusted to 5 mg of total protein in 1 mL of extract. Equal 500 μ L samples were incubated with either a rabbit polyclonal for Hsp70 (Santa Cruz Biotechnology H-300) or Goat IgG (Santa Cruz Biotechnology sc-2028). Samples received 5 μ L of DMSO (1%) or 5 μ L of JG-98 or YM-01 (5 mmol/L), making the final JG-98/YM-01 concentration 50 μ mol/L. Samples were gently rotated overnight at 4°C, followed by a 4-hour incubation with protein A/G-Sepharose Beads (Santa Cruz Biotechnology). The immunocomplexes were subjected to centrifugation at 1,000 \times g, washed three times with PBS pH 7.4, and eluted with SDS loading dye. Samples were separated on a 4% to 15% Tris-Tricine gel (Bio-Rad) and transferred to nitrocellulose membrane. The membranes were blocked in nonfat milk (5% milk in TBS, 0.1% Tween) for 1 hour, incubated with primary antibodies for Hsp70 (Santa Cruz Biotechnology sc-137239) and Bag3 (Santa Cruz Biotechnology sc-136467) overnight at 4°C, washed, and then incubated with a horseradish peroxidase-conjugated secondary antibody (Anaspec) for 1 hour. Finally, membranes were

developed using chemiluminescence (Thermo Scientific, Super-signal West Pico).

Animal toxicity study

NSG mice, which are often used for multiple myeloma studies, were dosed twice a week (Monday and Thursday) for 2 weeks with JG-98 or PBS:DMSO 1:1 vehicle (100 μ L) intraperitoneally. Body weights were measured every 2 days and mice were closely monitored for any signs of toxicity or discomfort. Twenty-four hours after the final dose, blood samples (300 μ L) were collected for plasma by cardiac puncture and sent for comprehensive chemistry analysis.

Pharmacokinetics

NSG mice (three per group) were dosed with 100 μ L of JG-98 or PBS:DMSO 1:1 vehicle solution intraperitoneally. Blood samples were collected for plasma through tail vein at 1, 3, 8, and 24-hour time points. JG-98 concentrations in plasma were determined by LC-MS, using a published protocol (24).

Xenografts

The antitumor efficacy of JG-98 was tested in nude mice as previously described (12). Briefly, one million MCF7 or HeLa cells in Matrigel were subcutaneously injected bilaterally into 6-week-old NCR mice (Taconic). Once tumors were established, JG-98 (3 mg/kg; $n = 5$) or a vehicle control (1:1 PBS:DMSO; $n = 5$) was introduced interperitoneally on days 2, 4, and 6. Tumor growth (10 tumors/5 mice) was measured by caliper every other day. The plots in Fig. 5 show the average tumor volumes and the error bars represent the SEM.

Results

Analysis of the Hsp70–Bag3 complex and selection of JG-98 as a possible chemical probe

Bag3 binds to the NBD of Hsp70, releasing client proteins from the chaperone and counteracting proteasome-mediated degradation (refs. 28, 29; Fig. 1A). Based on homology to other Bag domain-containing proteins (30), Bag3 is predicted to interact with the IB and IIB subdomains of Hsp70 (Fig. 1B). However, the

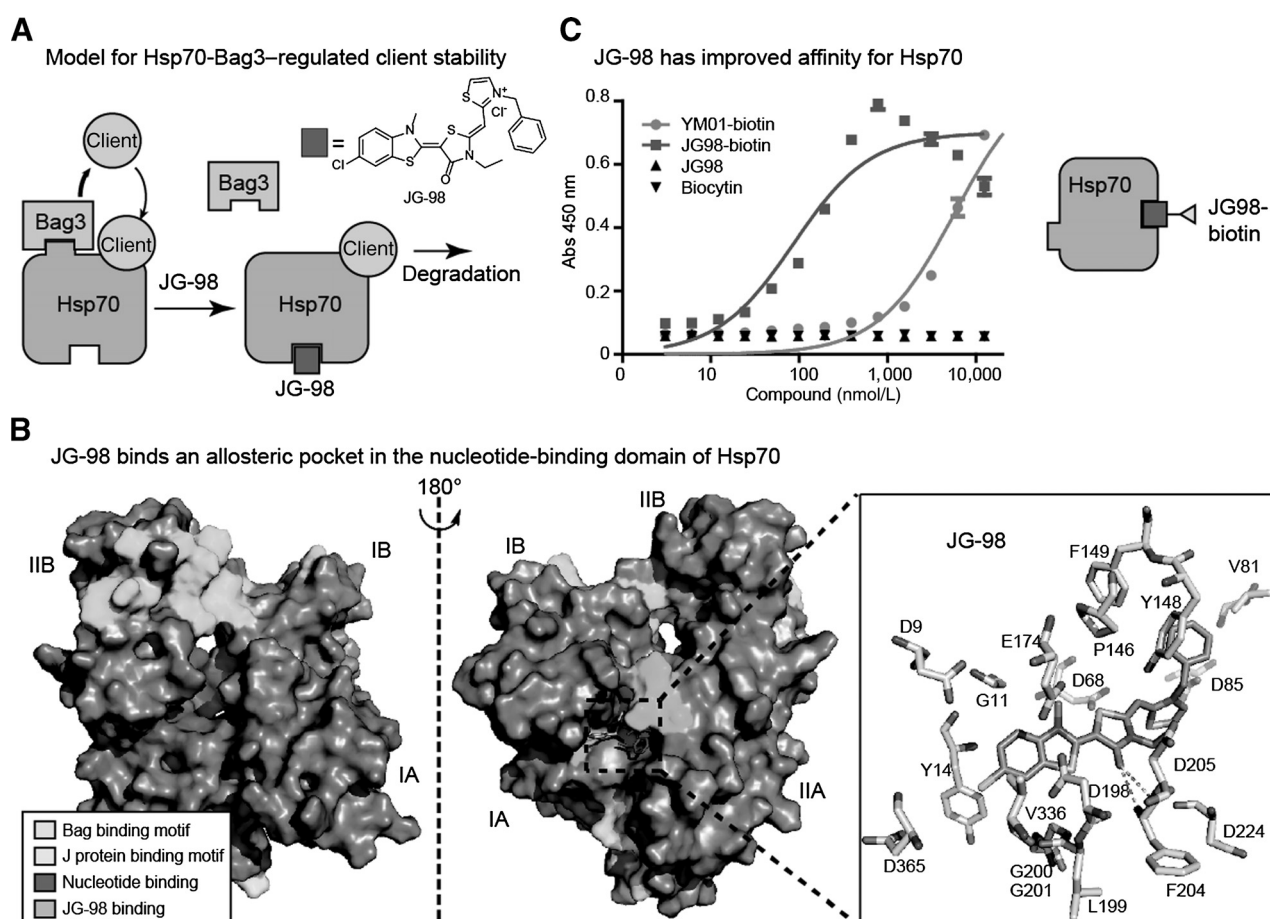
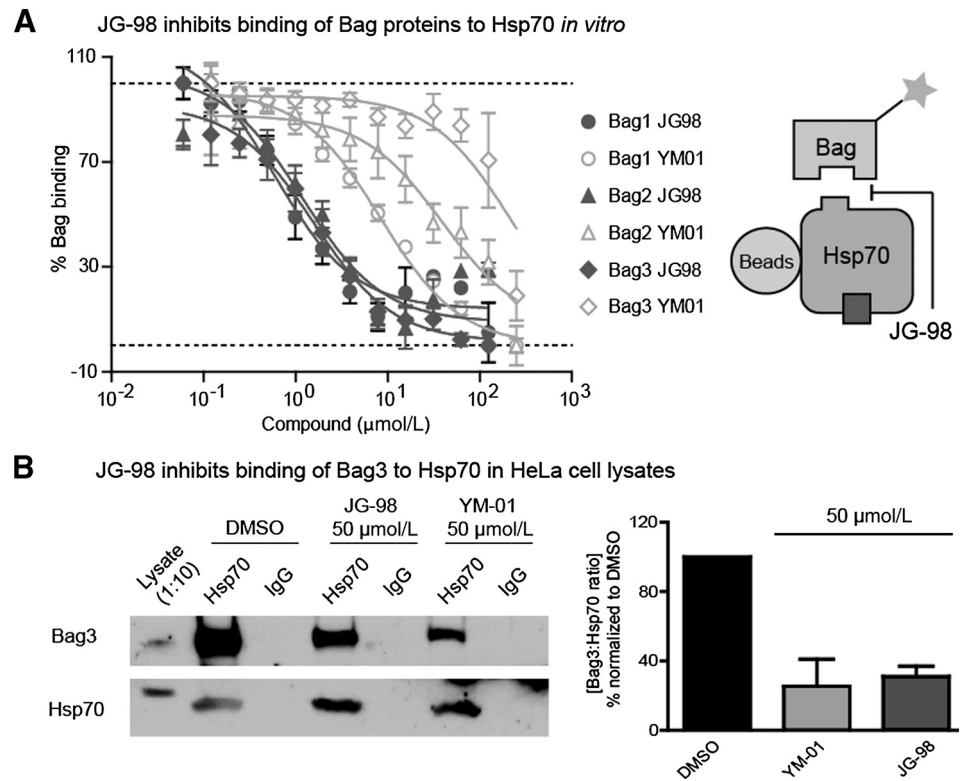


Figure 1.

JG-98 is an improved allosteric inhibitor of Hsp70. A, model for how Bag3 protects clients from degradation by releasing them from the Hsp70 complex. In this model, JG-98 is predicted to enhance turnover of cancer signaling proteins by blocking Bag3 binding to Hsp70. See the text for details. B, JG-98 binds in an allosteric pocket in the NBD of Hsp70. This site does not overlap with the nucleotide-binding cleft, the Bag3-interaction motif, or other PPI regions. The subdomains (IA, IIA, IB, and IIB) are labeled, and a close-up of the JG-98-binding pocket with the docked pose of compound is shown. C, JG-98 binds to purified Hsp70, as measured by ELISA. A schematic of the method is shown for clarity. Results are the average of at least three independent replicates performed in triplicate each. Error bars, SEM.

Figure 2.

JG-98 is an improved inhibitor of the PPI between Hsp70 and Bag3. A, JG-98 blocks the interaction of immobilized Hsp70 with labeled Bag3, as measured by flow cytometry. Results are the average of three independent experiments performed in triplicate. Error bars, SEM and some bars are smaller than the symbols. The positive control is an excess of unlabeled Hsp70 and the negative control is DMSO. B, JG-98 inhibits the Bag3–Hsp70 interaction by coimmunoprecipitation. Hsp70 was immunoprecipitated and blotted for bound Bag3. The blot is representative of experiments performed in triplicate and the quantification is an average of these experiments. Error bars, SEM.



affinity of the Hsp70–Bag3 interaction is significantly weakened (13-fold) in the presence of ADP (29), suggesting that stabilizing the ADP-bound state of Hsp70 might be one way of allosterically blocking the Hsp70–Bag3 contact. Coincidentally, we recently identified a chemical series, exemplified by YM-01 and JG-98 (Fig. 1A), that binds to Hsp70 and stabilizes it in the ADP-bound form (31). Thus, molecules in this series might be expected to destabilize the Hsp70–Bag3 interaction (Fig. 1A).

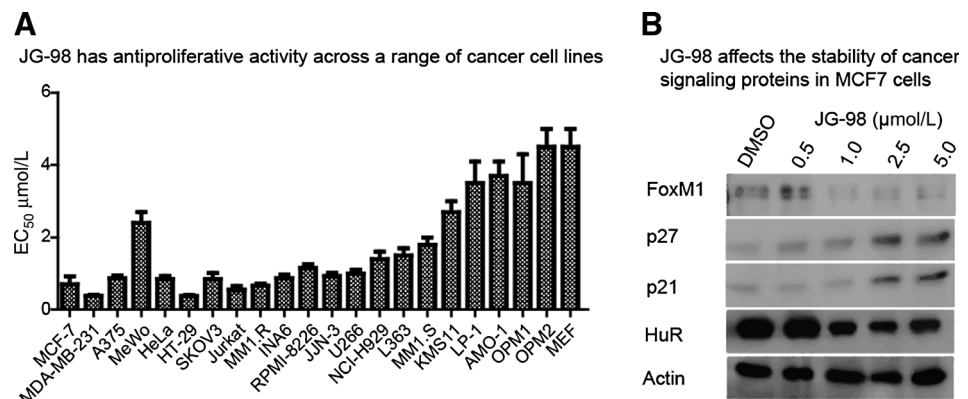
JG-98 binds tightly to Hsp70 and takes advantage of a previously unexplored pocket

To understand how JG-98 might impact the Hsp70–Bag3 interaction, we first docked JG-98 into an open conformation (see the Materials and Methods) of the highly conserved isoform Hsc70 (HSPA8; pdb: 3C7N). This docking was based on the known binding site of JG-98 that was previously deter-

mined by TROSY-HSQC NMR (24, 27). In the best-predicted models, JG-98 was anchored in a deep pocket (Fig. 1B) formed by residues G11, Y14, L199, G200, G201, and V336 in the NBD of Hsc70. These residues appeared to provide favorable hydrophobic interactions with the benzothiazole. Nearby residues were enriched in negatively charged amino acids, including D9, D68, D85, E174, D198, D205, D224, and D365, which seemed to provide favorable electrostatic interactions with the delocalized cation. Finally, the carbonyl in the central ring appeared to form hydrogen bonds with backbone amides in F204 and D205. The benzyl group in JG-98, which is not present in YM-01, reached into an adjacent pocket formed by V81, P146, Y148, and F149. Importantly, this binding site was not overlapping with the nucleotide-binding cassette, the Bag interaction motif or the sites of other PPIs in Hsp70 (Fig. 1B), supporting the allosteric activity of JG-98.

Figure 3.

JG-98 has antiproliferative activity. A, results of antiproliferative assays performed on a panel of cancer cell lines. Results are the average of at least two independent experiments performed in triplicate each. Error bars, SEM. B, JG-98 affects cancer signaling proteins previously linked to Hsp70–Bag3. It reduced FoxM1 and HuR and increased p21 and p27. Results are representative of experiments performed in triplicate.



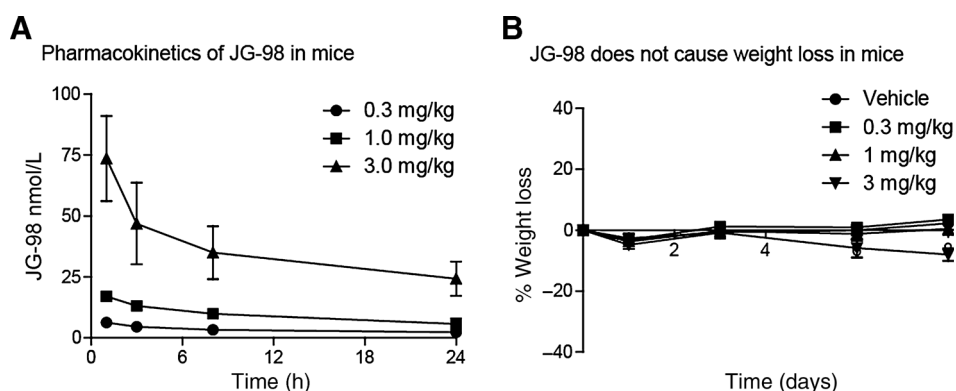


Figure 4. Pharmacokinetics and tolerability of JG-98 in mice. JG-98 was delivered intraperitoneally as described in the text. A, pharmacokinetics of JG-98 at three doses. Key parameters were calculated using PKSolver. B, no significant weight loss was observed in treated mice under these conditions. Three mice were used for each treatment group. Error bars, SEM.

The finding that JG-98 made additional contacts with V81, P146, Y148, and F149 suggested that JG-98 might bind tighter to Hsp70 than YM-01. To test this idea, we synthesized biotinylated versions of YM-01 and JG-98 (see Supplementary Fig. S1) and tested their direct binding to immobilized Hsp70 using an ELISA. The results showed that JG98-biotin (K_D of 86 ± 15 nmol/L) binds 60-fold tighter than YM01-biotin (K_D of $5,800 \pm 700$ nmol/L; Fig. 1C).

JG-98 interrupts the Hsp70–Bag3 PPI *in vitro* and in cells

Next, we tested whether JG-98 could block the Hsp70–Bag3 interaction *in vitro* using a flow cytometry protein interaction assay. In this approach, Hsp70 was immobilized on beads and we measured its binding to fluorescently labeled Bag3. The results showed that JG-98 strongly inhibited the interactions between Hsp70 and Bag3, with an IC_{50} value of 1.6 ± 0.3 μ mol/L, which was significantly better than YM-01 (IC_{50} value >100 ; Fig. 2A). Because the Bag domain is conserved in the related family members, Bag1 and Bag2, we also tested whether JG-98 and YM-01 could inhibit these PPIs. Consistent with the Bag3 results, JG-98 was a good inhibitor of the Hsp70–Bag1 and Hsp70–Bag2 complexes, with IC_{50} values of 0.6 ± 0.1 and 1.2 ± 0.1 μ mol/L, respectively (Fig. 2A); whereas YM-01 inhibited these interactions with IC_{50} values of 8.4 ± 0.8 and 39 ± 4 μ mol/L, respectively.

To test whether JG-98 could disrupt the Hsp70–Bag3 interaction in cells, Hsp70 was immunoprecipitated from HeLa cells in

the presence of JG-98 (50 μ mol/L), YM-01 (50 μ mol/L), or a DMSO vehicle control, and immunoblotted for Bag proteins. Both JG-98 and YM-01 reduced the Hsp70–Bag3 interaction by approximately 60% (Fig. 2B and Supplementary Fig. S2).

JG-98 inhibited growth of cancer cells by disrupting Hsp70–Bag3 function

The cytotoxic effects of JG-98 were then evaluated in a panel of cells derived from breast, cervical, skin, ovarian, and bone marrow cancers (Supplementary Fig. S3). Each of the cell lines was exposed to JG-98 for 72 hours and EC_{50} values were determined using an MTT cell proliferation assay. JG-98 was active against all of the lines tested, but the EC_{50} values were variable (between ~ 0.3 μ mol/L and 4 μ mol/L; Fig. 3A). Normal MEFs were relatively less sensitive (EC_{50} 4.5 ± 0.5 μ mol/L), but so were a number of multiple myeloma-derived cell lines, such as OPM1 and OPM2. It is not yet clear why some cells are more/less sensitive, but the submicromolar activity against a subset of cancer lines, including MCF7 and HeLa, was encouraging.

The Hsp70–Bag3 complex is known to regulate cancer cell metastasis and survival through multiple pathways, including through the FoxM1 and HuR transcription factors (12). Consistent with this role, treatment with JG-98 reduced the levels of FoxM1 and HuR, while increasing the levels of the cell-cycle inhibitors, p27 and p21, in MCF7 breast cancer cells (Fig. 3B). This effect mirrors what is seen upon Bag3 knockdown in these cells (12).

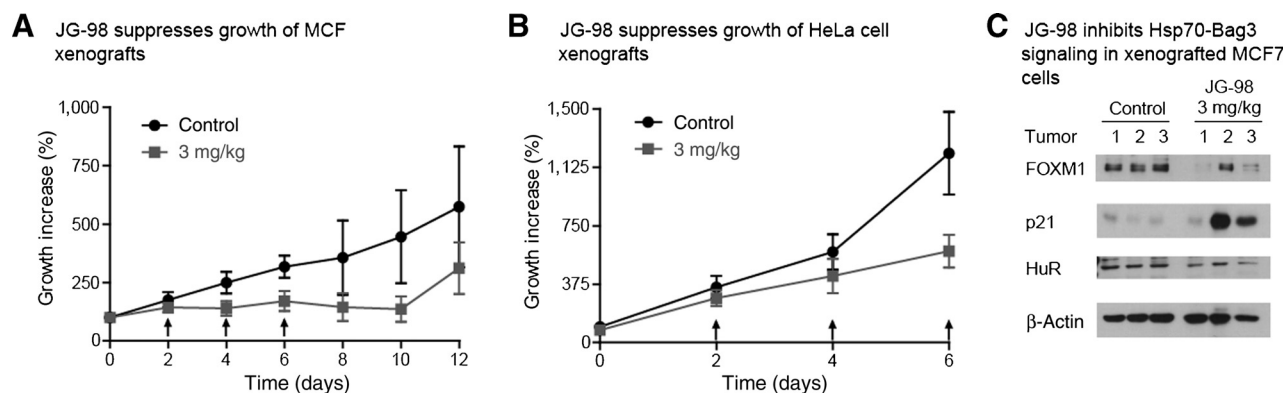


Figure 5. JG-98 is active in MCF7 and HeLa xenograft models. JG-98 treatment of mice with either MCF7 cells (A) or HeLa cells (B) xenografted. See the Materials and Methods for experimental details. Arrows, treatments with JG-98. C, treated samples from A were isolated, and the levels of select signaling proteins were measured by Western blot analyses for three separate animals.

Evaluation of JG-98 pharmacokinetics and toxicity in mice

Next, we wanted to use JG-98 as a probe to explore the Hsp70–Bag3 complex in mice. JG-98 was administered through intraperitoneal injection twice a week for 2 weeks with three different doses (0.3, 1, and 3 mg/kg) in NSG mice. The doses were given in 1:1 DMSO:PBS, which served as the vehicle control. After the final dose, blood samples were collected and JG-98 concentrations in the plasma were evaluated. By high-performance liquid chromatography, the levels of JG-98 reached approximately 70 nmol/L in plasma after 1 hour at the 3 mg/kg dose (Fig. 4A and Supplementary Fig. S3A). Care must be taken in interpreting these findings because precursors of JG-98 are known to accumulate at 100-fold higher concentrations in tumor cells *in vivo* (32). At all three doses, the terminal half-life was calculated to be approximately 20 hours (Fig. 4A and Supplementary Fig. S4A).

An early analog in this series, MKT-077, was abandoned in phase I clinical trials due to its renal accumulation (33). Thus, we wanted to pay special attention to the potential toxicity of JG-98. No significant weight loss (<10%) was observed in treated animals (Fig. 4B). After the final dose, blood samples were also collected and screened for biomarkers of liver and renal function. We found that blood urea nitrogen and creatinine levels were normal at all three dosages, indicating that renal function was unimpaired (Supplementary Fig. S4B). Similarly, markers of liver function, alanine aminotransferase and total bilirubin, were in the normal range (Supplementary Fig. S4B).

JG-98 is active against MCF7 and HeLa cells in xenograft models

To test the efficacy of JG-98 *in vivo*, xenografts of MCF7 cells were established in nude mice and, after tumors reached 100 mm³, compound was administered intraperitoneally on days 0, 2, and 4. We found that a dosage of 3 mg/kg limited tumor growth until day 6 (Fig. 5A), but tumors appeared to resume growing following the end of drug administration. Similarly, JG-98 (3 mg/kg) suppressed tumor growth in a HeLa xenograft model, though somewhat less effectively (Fig. 5B). When tumor samples from the MCF7 xenograft study were homogenized and tested for effects on cancer signaling markers, the results resembled what was seen in cultured MCF7 cells; specifically, p21 was significantly elevated, while HuR and FoxM1 tended to be decreased (Fig. 5C). Together, these proof-of-concept results suggest that the Hsp70–Bag3 PPI may be a promising target for further exploration.

Discussion

In the ongoing search for new cancer targets, a number of promising PPIs have emerged (17, 18). In addition, allosteric inhibitors have made it possible to block PPIs that are seemingly difficult to target by exploiting deep binding pockets located far from the site of the protein–protein contact (20). In this work, we used an allosteric inhibitor of the Hsp70–Bag3 interaction, JG-98, to study whether this PPI might be a new drug target. We found that JG-98 interrupted the Hsp70–Bag3 interaction *in vitro* and in cells. JG-98 was significantly more effective than YM-01 at this

task, likely because it was able to access a previously underexplored set of contacts near the allosteric-binding pocket. Furthermore, JG-98 was more stable than YM-01 in animals, making it a suitable chemical probe for studying the importance of the Hsp70–Bag3 complex *in vivo*.

We found that JG-98 affected the stability of multiple signaling proteins that had previously been linked to the Hsp70–Bag3 complex. Specifically, we noted that treatment with JG-98 caused loss of FoxM1 and HuR, with a corresponding increase in p21 and p27. How does this occur? It is possible that Bag3 normally suppresses Hsp70-mediated degradation of FoxM1 and HuR (as in Fig. 1A). Thus, inhibition of Bag3 binding would be expected to accelerate the turnover of these proteins. However, it is also very important to note that, in addition to the proteins studied here, other pathways are likely to contribute to the antiproliferative activity of JG-98. For example, the complex between Hsp70 and Bag1 has been linked to regulation of Raf1/ERK (34), so it is likely that treatment with JG-98 would impact cytoskeletal dynamics, invasion, and other pathways (11). An understanding of the full scope of mechanisms linking Hsp70 and Bag family members to cell death will require additional studies. We suggest that these inquiries will be greatly facilitated by the availability of JG-98.

Disclosure of Potential Conflicts of Interest

J.S. Weissman has an immediate family member who is Head of Cancer Signaling for Roche, reports receiving a commercial research grant from Onyx, and has ownership interest (including patents) in Driver. No potential conflicts of interest were disclosed by the other authors.

Authors' Contributions

Conception and design: X. Li, T. Colvin, J.S. Weissman, M.Y. Sherman, J.E. Gestwicki

Development of methodology: X. Li, T. Colvin, B. Donyak, B. Hann, M. Cho, J.S. Weissman

Acquisition of data (provided animals, acquired and managed patients, provided facilities, etc.): X. Li, T. Colvin, J.N. Rauch, D. Acosta-Alvear, B. Donyak, B. Hann, B.T. Aftab, M. Murnane, M. Cho, P. Walter

Analysis and interpretation of data (e.g., statistical analysis, biostatistics, computational analysis): X. Li, T. Colvin, D. Acosta-Alvear, M. Kampmann, B. Donyak, B.T. Aftab, M. Murnane, M. Cho, P. Walter, M.Y. Sherman, J.E. Gestwicki

Writing, review, and/or revision of the manuscript: X. Li, B. Donyak, B.T. Aftab, M.Y. Sherman, J.E. Gestwicki

Study supervision: P. Walter, M.Y. Sherman, J.E. Gestwicki

Other (potency determination in multiple myeloma cell panel): B.T. Aftab

Grant Support

This work was funded by the Steven and Nancy Grand Multiple Myeloma Translational Initiative (to B.T. Aftab), the Howard Hughes Medical Institute (to J.E. Gestwicki, P. Walter, and J.S. Weissman), and funds from NIH CA081244 (to M.Y. Sherman), NS059690 (to J.E. Gestwicki), and K99CA181494 (to M. Kampmann).

The costs of publication of this article were defrayed in part by the payment of page charges. This article must therefore be hereby marked *advertisement* in accordance with 18 U.S.C. Section 1734 solely to indicate this fact.

Received August 22, 2014; revised December 15, 2014; accepted December 16, 2014; published OnlineFirst January 6, 2015.

References

- Hartl FU, Bracher A, Hayer-Hartl M. Molecular chaperones in protein folding and proteostasis. *Nature* 2011;475:324–32.
- Wisén S, Bertelsen EB, Thompson AD, Patury S, Ung P, Chang L, et al. Binding of a small molecule at a protein-protein interface regulates

- the chaperone activity of Hsp70-Hsp40. *ACS Chem Biol* 2010;5: 611–22.
3. Powers MV, Clarke PA, Workman P. Dual targeting of Hsc70 and HSP72 inhibits HSP90 function and induces tumor-specific apoptosis. *Cancer Cell* 2008;14:250–62.
 4. Massey AJ, Williamson DS, Browne H, Murray JB, Dokurno P, Shaw T, et al. A novel, small molecule inhibitor of Hsc70/Hsp70 potentiates Hsp90 inhibitor induced apoptosis in HCT116 colon carcinoma cells. *Cancer Chemother Pharmacol* 2010;66:535–45.
 5. Evans CG, Chang L, Gestwicki JE. Heat Shock Protein 70 (Hsp70) as an emerging drug target. *J Med Chem* 2010;53:4585–602.
 6. Kang Y, Taldone T, Patel HJ, Patel PD, Rodina A, Gozman A, et al. Heat shock protein 70 inhibitors. 1. 2,5'-Thiodipyrimidine and 5-(phenylthio)pyrimidine acrylamides as irreversible binders to an allosteric site on heat shock protein 70. *J Med Chem* 2014;57:1188–207.
 7. Taldone T, Kang Y, Patel HJ, Patel MR, Patel PD, Rodina A, et al. Heat shock protein 70 inhibitors. 2. 2,5'-Thiodipyrimidines, 5-(phenylthio)pyrimidines, 2-(pyridin-3-ylthio)pyrimidines, and 3-(Phenylthio)pyridines as reversible binders to an allosteric site on Heat Shock Protein 70. *J Med Chem* 2014;57:1208–24.
 8. Leu JJJ, Pimkina J, Frank A, Murphy ME, George DL. A small molecule inhibitor of inducible heat shock protein 70. *Mol Cell* 2009;36: 15–27.
 9. Assimon VA, Gillies AT, Rauch JN, Gestwicki JE. Hsp70 protein complexes as drug targets. *Curr Pharm Des* 2013;19:404–17.
 10. Franceschelli S, Rosati A, Lerosé R, De Nicola S, Turco MC, Pascale M. bag3 gene expression is regulated by heat shock factor 1. *J Cell Physiol* 2008;215:575–7.
 11. Rosati A, Graziano V, De Laurenzi V, Pascale M, Turco MC. BAG3: a multifaceted protein that regulates major cell pathways. *Cell Death Dis* 2011;2:e141.
 12. Colvin TA, Gabai VL, Gong J, Calderwood SK, Li H, Gummuluru S, et al. Hsp70-Bag3 interactions regulate cancer-related signaling networks. *Cancer Res* 2014;74:4731–40.
 13. Vassilev LT, Vu BT, Graves B, Carvajal D, Podlaski F, Filipovic Z, et al. *In vivo* activation of the p53 pathway by small-molecule antagonists of MDM2. *Science* 2004;303:844–8.
 14. Chene P. Inhibition of the p53-MDM2 interaction: targeting a protein-protein interface. *Mol Cancer Res* 2004;2:20–8.
 15. Abulwerdi F, Liao C, Liu M, Azmi AS, Aboukameel A, Mady ASA, et al. A novel small-molecule inhibitor of Mcl-1 blocks pancreatic cancer growth *in vitro* and *in vivo*. *Mol Cancer Ther* 2014;13:565–75.
 16. Oltersdorf T, Elmore SW, Shoemaker AR, Armstrong RC, Augeri DJ, Belli BA, et al. An inhibitor of Bcl-2 family proteins induces regression of solid tumours. *Nature* 2005;435:677–81.
 17. Arkin MR, Wells JA. Small-molecule inhibitors of protein-protein interactions: progressing towards the dream. *Nat Rev Drug Discov* 2004; 3:301–17.
 18. Ivanov AA, Khuri FR, Fu H. Targeting protein-protein interactions as an anticancer strategy. *Trends Pharmacol Sci* 2013;34:393–400.
 19. Smith MC, Gestwicki JE. Features of protein-protein interactions that translate into potent inhibitors: topology, surface area and affinity. *Expert Rev Mol Med* 2012;14:e16.
 20. Thompson AD, Dugan A, Gestwicki JE, Mapp AK. Fine-tuning multiprotein complexes using small molecules. *ACS Chem Biol* 2012;7:1311–20.
 21. Wells JA, McClendon CL. Reaching for high-hanging fruit in drug discovery at protein-protein interfaces. *Nature* 2007;450:1001–9.
 22. Xu Z, Page RC, Gomes MM, Kohli E, Nix JC, Herr AB, et al. Structural basis of nucleotide exchange and client binding by the Hsp70 cochaperone Bag2. *Nat Struct Mol Biol* 2008;15:1309–17.
 23. Sondermann H, Scheufler C, Schneider C, Höfheld J, Hartl F-U, Moarefi I. Structure of a Bag/Hsc70 complex: convergent functional evolution of Hsp70 nucleotide exchange factors. *Science* 2001;291:1553–7.
 24. Li X, Srinivasan SR, Connarn J, Ahmad A, Young ZT, Kabza AM, et al. Analogues of the allosteric heat shock protein 70 (Hsp70) inhibitor, MKT-077, as anti-cancer agents. *ACS Med Chem Lett* 2013;4:1042–7.
 25. McMillin DW, Delmore J, Weisberg E, Negri JM, Geer DC, Klippel S, et al. Tumor cell-specific bioluminescence platform to identify stroma-induced changes to anticancer drug activity. *Nat Med* 2010;16:483–9.
 26. McMillin DW, Jacobs HM, Delmore JE, Buon L, Hunter ZR, Monroe V, et al. Molecular and cellular effects of NEDD8-activating enzyme inhibition in myeloma. *Mol Cancer Ther* 2012;11:942–51.
 27. Rousaki A, Miyata Y, Jinwal UK, Dickey CA, Gestwicki JE, Zuideker ERP. Allosteric drugs: the interaction of antitumor compound MKT-077 with human Hsp70 chaperones. *J Mol Biol* 2011;411:614–32.
 28. Doong H, Rizzo K, Fang S, Kulpa V, Weissman AM, Kohn EC. CAIR-1/BAG-3 abrogates heat shock protein-70 chaperone complex-mediated protein degradation: accumulation of poly-ubiquitinated Hsp90 client proteins. *J Biol Chem* 2003;278:28490–500.
 29. Rauch JN, Gestwicki JE. Binding of human nucleotide exchange factors to heat shock protein 70 (Hsp70) generates functionally distinct complexes *in vitro*. *J Biol Chem* 2014;289:1402–14.
 30. Takayama S, Xie Z, Reed JC. An evolutionarily conserved family of Hsp70/Hsc70 molecular chaperone regulators. *J Biol Chem* 1999;274:781–6.
 31. Wang AM, Miyata Y, Klinedinst S, Peng H-M, Chua JP, Komiyama T, et al. Activation of Hsp70 reduces neurotoxicity by promoting polyglutamine protein degradation. *Nat Chem Biol* 2013;9:112–8.
 32. Tatsuta N, Suzuki H, Mochizuki T, Koya K, Kawakami M, Shishido T, et al. Pharmacokinetic analysis and antitumor efficacy of MKT-077, a novel antitumor agent. *Cancer Chemother Pharmacol* 1999;43:295–301.
 33. Propper DJ, Braybrooke JP, Taylor DJ, Lodi R, Styles P, Cramer JA, et al. Phase I trial of the selective mitochondrial toxin MKT 077 in chemoresistant solid tumours. *Ann Oncol* 1999;10:923–7.
 34. Song J, Takeda M, Morimoto RI. Bag1-Hsp70 mediates a physiological stress signalling pathway that regulates Raf-1/ERK and cell growth. *Nat Cell Biol* 2001;3:276–82.